

Deterministic generation of cat states with more than 100 photons under dissipation

Zhu-yao Jin¹ and Jun Jing^{1,*}

¹*School of Physics, Zhejiang University, Hangzhou 310027, Zhejiang, China*

(Dated: June 3, 2026)

Large-size cat states are especially meaningful and fundamental for exploring the quantum-to-classical transition, as well as promising resources for quantum metrology and fault-tolerant quantum computation. However, amplifying the magnitude of cat states remains challenging because of the growing fragility under decoherence. We propose to generate large cat states by using the dynamical invariant of hybrid qubit-bosonic systems under Hermitian or non-Hermitian time-dependent Hamiltonian. It is a study with the universal quantum control (UQC) theory, in which the system dynamics is analyzed in the ancillary picture via a unitary transformation conditional on the qubit state. The controllable dynamics that can be encoded in the evolution of the dynamical invariant is presented by the Heisenberg equation, which imposes constraints on the Hamiltonian. When the qubit is prepared in a balanced superposed state, the bosonic mode can evolve deterministically from the vacuum state to the cat state of a mean photon number over 120. In the Hermitian case, the generation is perfect; and in the non-Hermitian case, the fidelity is over 0.962. Our protocol can also be applied to the generation of the intrinsic cat states and the four-component cat states of large size. Through the preparation of macroscopic quantum states, our work essentially advances UQC to hybrid discrete-continuous variable systems.

I. INTRODUCTION

The notion of the intrinsic cat states traces back to Schrödinger's gedanken experiment [1], where the cat's two macroscopically distinguished components or states, i.e., dead and alive, are respectively entangled with the radioactive decay process and the subsequent breaking of the poison bottle and the otherwise stable state. This paradigmatic model embarks the investigation of the macroscopic quantum states [2], expected to address the fundamental and open question concerning the boundary between classical and quantum worlds [2–5].

In literature, the macroscopic quantum states refer mainly to the atomic cat states [6–9] and the bosonic cat states [10, 11]. The size of the atomic cat states is characterized by the involved atomic number. However, their preparation in practice is hindered by the systematic errors and the dissipation on individual atoms [6–9], whose effect grows with the state size. The fidelities of the cat states observed in 20 Rydberg atoms [7] and in 20 superconducting qubits [8] are as low as 0.542 and 0.525, respectively. In comparison to atomic systems, bosonic modes provide a more versatile platform for generating cat states as superpositions of coherent states [10, 11]: $|\alpha\rangle + |-\alpha\rangle$. When $|\alpha| > 2$, the coherent bases are approximately orthogonal to each other and thereby cat state can be regarded as a macroscopic quantum state [12, 13]. Similar superposed states realized in the massive systems can also manifest the quantum macroscopicity [14]. Large-amplitude bosonic cat states constitute a foundation for exploring the quantum-to-classical transition [10, 11], the high-fidelity quantum teleportation [15, 16], the enhanced sensitivity of phase

estimation [17–20], and fault-tolerant quantum computation [21–27]. The bit-flip errors occurred on the cat qubits [24, 25] are found to be exponentially suppressed by the increasing amplitude of cat states [28, 29]. Large cat states have been observed in many systems, including the trapped-ion systems [30–35], the circuit QED (cQED) systems [25, 36–38] and the circuit quantum acoustodynamics systems [14], e.g., in cQED system [38], a cat state with amplitude $|\alpha| \sim \sqrt{7}$ and fidelity ~ 0.81 has been observed. And the optical cat states of the electromagnetic wave fields are reported with an amplitude $|\alpha| \sim 1.85$, a fidelity ~ 0.99 , and a success probability 0.2 [39].

Besides the two-legged cat states, the four-legged cat states or so-called compass states [24, 38, 40–46]: $|\alpha\rangle + |-\alpha\rangle + |i\alpha\rangle + |-i\alpha\rangle$ are more promising candidates for quantum technologies, such as quantum metrology [43], dark matter searching [44], and quantum error tracking and correction in the presence of photon loss [38, 41, 42]. Recently, a four-legged state has been demonstrated in a cQED system [44] with amplitude $|\alpha| \sim \sqrt{12}$ and fidelity > 0.95 , yet the success probability is lower than 0.01.

Existing theoretical protocols for the cat-state generation are diverse in their own advantages and constraints. The adiabatic protocol is based on slowly tuning the two-photon driving field of a Kerr-nonlinear resonator [47–49], whose capability is severely limited by the prolonged exposure to the environment. To overcome this limitation, the evolution process [49] can be accelerated by the shortcuts to adiabaticity (STA) [49, 50] via an extra two-photon driving field. The attainable cat-state amplitude is about $|\alpha| < 2$, subject to the ratio of ancillary driving strength and the Kerr nonlinearity [25, 51]. In the Jaynes-Cummings model under two-photon driving field [52], STA demonstrates in theory a cat state with $|\alpha| \sim 2$ in a highly squeezed frame with a squeezing level as high as ~ 15 dB. This level is hardly accessible in ex-

* Contact author: jingjun@zju.edu.cn

periments. In addition, by combining a quantum gate that transfers an arbitrary state of a qubit into a superposition of two quasiorthogonal coherent states with opposite phases of a cavity-mode [38, 41, 42, 53] with sequential pulses on qubit and cavity, one can deterministically generate a cat state with amplitude $|\alpha| \sim \sqrt{7}$ and fidelity ~ 0.91 [41]. Using the photon subtraction method [39, 54–59] on a squeezed vacuum state with a squeezing level above 15 dB [58], a large cat state was predicted with $|\alpha| \sim \sqrt{10}$ and fidelity > 0.99 [58], yet the protocol is probabilistic with a success probability ~ 0.02 . As for steady states, stabilization of cat states of a high fidelity requires the two-photon loss rate to dominate the single-photon loss rate [60–62]. In both theory and experiment, it is generally hard to create large cat states in open quantum systems [24, 63]. A unified theoretical framework for both closed and open quantum systems is desired for deterministically generating the large-size cat states with accessible control.

Our universal quantum control (UQC) framework [64–68] provides a much broader perspective for controlling the dynamics of classical systems [68] and both discrete-variable and continuous-variable quantum systems of Hermitian or non-Hermitian Hamiltonian [64–68]. Fundamentally it is based on the dynamical invariants of systems, which are constructed through the gauge potential induced by representation transformation. In this paper, for deterministic generation of the large-amplitude cat states, we construct the dynamical invariants for the hybrid qubit-bosonic systems, where the qubit is longitudinally coupled to the bosonic system. For the Hermitian systems, a dynamical invariant is constructed to satisfy the Heisenberg equation with the rotated Hamiltonian, giving rise to the constraint conditions on the original Hamiltonian. When the qubit is initially in the balanced superposed state and the bosonic mode is in the vacuum state, the mode can evolve to a cat state with unit fidelity and mean photon number ~ 120 . For the open quantum systems, the dynamical invariant satisfies the Heisenberg equation with the non-Hermitian Hamiltonian, it imposes the constraint conditions associated with the gain and loss rates. Under the conditional probability conservation, it is found that the cat states can be deterministically generated with a fidelity $\mathcal{F} > 0.962$ and a mean photon number ~ 120 . Moreover, our protocol is applied to the generation of the intrinsic cat states and the four-legged cat states with record high fidelity and amplitudes.

The rest of this paper is structured as follows. The UQC theory is briefly recalled in Secs. II A and II B for the Hermitian and non-Hermitian systems, respectively, demonstrating controllable system dynamics via dynamical invariants. In Sec. III, we apply the general theory to the closed hybrid qubit-bosonic systems and construct the relevant dynamical invariant to generate large-amplitude cat states. In Sec. IV, the general theory is extended to the open hybrid qubit-bosonic systems, whose dynamics is described by the non-Hermitian

Hamiltonian. Our protocol is extended in Secs. V A and V B to the generation of the large-amplitude intrinsic cat states and four-legged cat states, respectively. The entire work is summarized in Sec. VI. Appendix A details the derivation for the non-Hermitian Hamiltonian of the hybrid qubit-bosonic systems from the Lindblad master equation.

II. UNIVERSAL QUANTUM CONTROL THEORY

This section briefly outlines the spirit of the universal quantum control theory [64–68] for the time-dependent systems, Hermitian or non-Hermitian. This framework substantially demonstrates the controllable system dynamics via the dynamical invariants and the gauge potential. The gauge potential can be introduced by the geometric transformation between the time-dependent and the time-independent ancillary representations.

A. Hermitian systems

In the Hermitian case, the system dynamics is generally described by the Schrödinger equation as ($\hbar \equiv 1$)

$$i \frac{\partial}{\partial t} |\psi(t)\rangle = H(t) |\psi(t)\rangle, \quad (1)$$

with the time-dependent Hamiltonian $H(t)$ and the pure-state solution $|\psi(t)\rangle$. Although the solutions to Eq. (1) can be in principle obtained from the instantaneous eigenvalue equations, such a brute-force approach will become increasingly intractable as the system size grows.

Alternatively, the system dynamics can be described in the ancillary representation via a time-dependent unitary transformation $\mathcal{V}(t)$ [64–68]. In the relevant rotating frame, the system Hamiltonian is transformed as

$$H_{\text{rot}}(t) = \mathcal{V}^\dagger(t) H(t) \mathcal{V}(t) - i \mathcal{V}^\dagger(t) \frac{\partial \mathcal{V}(t)}{\partial t}, \quad (2)$$

where the second term describes the holonomic contribution in the Hilbert space [69] or the gauge potential determined by $\mathcal{V}(t)$. One can impose constraints on the rotated Hamiltonian (2) by requiring the stationary dynamical invariants $\mathcal{J}(0)$ to satisfy the Heisenberg equation as [68]:

$$\frac{\partial \mathcal{J}(0)}{\partial t} = -i [H_{\text{rot}}(t), \mathcal{J}(0)], \quad (3)$$

where $\mathcal{J}(0) = \tilde{\mu}(0), \tilde{\mu}^\dagger(0)$ can be accompanied with a real-valued gauge-invariant global phase $f(t)$, e.g., $\tilde{\mu}(0) \equiv \exp[i f(t)] \mu(0)$. In the continuous-variable systems [68], $\mu(0)$ and $\mu^\dagger(0)$ are the ancillary operators superposed of the bosonic operators in the original picture.

In accordance with Eq. (3), we can have time-dependent dynamical invariants $\mathcal{J}(t) = \tilde{\mu}(t), \tilde{\mu}^\dagger(t)$,

where $\tilde{\mu}(t) = \mathcal{V}(t)\tilde{\mu}(0)\mathcal{V}^\dagger(t)$, satisfying the Heisenberg equation with the original Hamiltonian (1). Particularly under the inversion of Eq. (2), Eq. (3) is transformed as

$$\begin{aligned} \frac{\partial[\mathcal{V}^\dagger(t)\mathcal{J}(t)\mathcal{V}(t)]}{\partial t} &= -i\left[\mathcal{V}^\dagger(t)H(t)\mathcal{V}(t) \right. \\ &\left. - i\mathcal{V}^\dagger(t)\frac{\partial\mathcal{V}(t)}{\partial t}, \mathcal{V}^\dagger(t)\mathcal{J}(t)\mathcal{V}(t)\right]. \end{aligned} \quad (4)$$

Using the chain rule, we have

$$\begin{aligned} \mathcal{V}^\dagger(t)\frac{\partial\mathcal{J}(t)}{\partial t}\mathcal{V}(t) &= -i\mathcal{V}^\dagger(t)[H(t), \mathcal{J}(t)]\mathcal{V}(t) \\ &+ \mathcal{V}^\dagger(t)\mathcal{J}(t)\frac{\partial\mathcal{V}(t)}{\partial t} - \mathcal{V}^\dagger(t)\frac{\partial\mathcal{V}(t)}{\partial t}\mathcal{V}^\dagger(t)\mathcal{J}(t)\mathcal{V}(t) \\ &- \frac{\partial\mathcal{V}^\dagger(t)}{\partial t}\mathcal{J}(t)\mathcal{V}(t) - \mathcal{V}^\dagger(t)\mathcal{J}(t)\frac{\partial\mathcal{V}(t)}{\partial t}. \end{aligned} \quad (5)$$

By left-multiplying Eq. (5) with $\mathcal{V}(t)$ and right-multiplying it with $\mathcal{V}^\dagger(t)$, and using the relation $d[\mathcal{V}(t)\mathcal{V}^\dagger(t)]/dt = [d\mathcal{V}(t)/dt]\mathcal{V}^\dagger(t) + \mathcal{V}(t)[d\mathcal{V}^\dagger(t)/dt] = 0$, it is ended up with

$$\frac{\partial\mathcal{J}(t)}{\partial t} = -i[H(t), \mathcal{J}(t)]. \quad (6)$$

This self-consistent proof confirms that under the constraints imposed on $H(t)$ by Eq. (6), the system dynamics can be described by the evolution of both two dynamical invariants:

$$\mu(0) \rightarrow e^{if(t)}\mu(t) \quad \& \quad \mu^\dagger(0) \rightarrow e^{-if(t)}\mu^\dagger(t). \quad (7)$$

In various formulations, the dynamical invariants render ubiquitous applications, covering both discrete-variable [64] and continuous-variable [66].

B. Non-Hermitian systems

Our theory based on the dynamical invariants and the gauge potential enables controllable dynamics of the open quantum systems driven by the non-Hermitian Hamiltonian [65, 67, 68].

For discrete-variable systems, the dynamics can be described by the non-Hermitian Hamiltonian that is derived from Lindblad master equation by ignoring the quantum jump terms under postselection [70]. In contrast, for the continuous-variable systems governed by the quadratic Hamiltonian, the non-Hermitian Hamiltonian can be rigorously derived from the adjoint Lindblad master equation with all the jump terms retained [67, 68, 71, 72]. In general, under the biorthogonal assumption [73], the dynamics of non-Hermitian systems can be described by two sets of time-dependent Schrödinger equation as

$$i\frac{\partial}{\partial t}|\psi(t)\rangle = H(t)|\psi(t)\rangle, \quad i\frac{\partial}{\partial t}\langle\phi(t)| = H^\dagger(t)\langle\phi(t)|, \quad (8)$$

with $H(t) \neq H^\dagger(t)$, and $|\psi(t)\rangle$ and $\langle\phi(t)|$ are the pure-state solutions in the ket and bra spaces, respectively.

Without loss of generality, we focus on the dynamics of the systems in the ket space governed by $H(t)$ in the following. Similar to the Hermitian case, in the rotating frame with respect to the unitary transformation $\mathcal{V}(t)$ [67, 68], the transformed Hamiltonian $H_{\text{rot}}(t)$ takes a similar form as Eq. (2). The dynamical component $\mathcal{V}^\dagger(t)H(t)\mathcal{V}(t)$ is non-Hermitian and the geometrical component $-i\mathcal{V}^\dagger\dot{\mathcal{V}}$ remains Hermitian. Thus the dynamical invariant $\mu(t)$ and its Hermitian conjugate $\mu^\dagger(t)$ cannot simultaneously satisfy the Heisenberg equation (6) under the same Hamiltonian. In other words, only one of $\mu(t)$ and $\mu^\dagger(t)$ can be activated as the universal passages for controlling the system dynamics [67, 68]. Accordingly, the system dynamics is effectively demonstrated as

$$\mu(0) \rightarrow e^{if(t)}\mu(t) \quad | \quad \mu^\dagger(0) \rightarrow e^{-if(t)}\mu^\dagger(t), \quad (9)$$

where $f(t)$ becomes a complex-valued global phase, in sharp contrast to Eq. (7). The imaginary part of $f(t)$ encodes gain or loss induced by the system-environment interaction, leading to the probability nonconservation of the system wave-function. By an appropriate choice of systematic parameters, $f(t)$ could become a real number at a predesigned moment t , corresponding to the automatic normalization of the system wave-function. Also, the non-Hermitian dynamical invariants has enabled perfect transfer of arbitrary states in both discrete-variable [65] and continuous-variable systems [67] and the generation of ultra highly squeezed states in open quantum systems [68]. Next, we extend the UQC theory [67, 68] to construct the dynamical invariants for a hybrid discrete-continuous variable system.

III. GENERATION OF CAT STATES IN CLOSED QUBIT-BOSONIC SYSTEMS

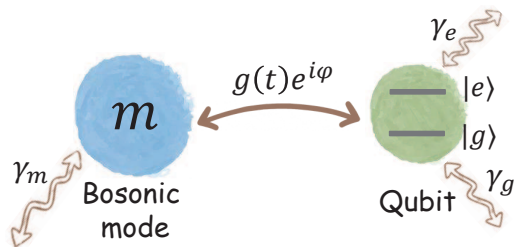


FIG. 1. Sketch of the open hybrid qubit-bosonic system, where the qubit is longitudinally coupled to the bosonic mode with the coupling strength $g(t)$ and the phase ϕ . γ_e , γ_g and γ_m denote the gain or loss rates of the levels $|e\rangle$ and $|g\rangle$ and the bosonic mode, respectively. When $\gamma_a = 0$, $a = e, g, m$, it reduces to a closed qubit-bosonic system.

Our study in this section is conducted on a closed hybrid quantum system consisting of a qubit and a bosonic mode as shown in Fig. 1 with vanishing gain or loss rates $\gamma_a = 0$, $a = e, g, m$. The qubit is composed of an excited state $|e\rangle$ and a ground state $|g\rangle$, which is coupled to the

bosonic mode by the longitudinal interaction with coupling strength $g(t)$ and phase φ . The Hamiltonian of the composite system can be expressed as

$$H(t) = \omega_m(t)m^\dagger m + \frac{\omega_q(t)}{2}\sigma_z + g(t)\sigma_z (me^{i\varphi} + m^\dagger e^{-i\varphi}), \quad (10)$$

where m (m^\dagger) denotes the annihilation (creation) operator of the bosonic mode, and the Pauli operator is defined as $\sigma_z \equiv |e\rangle\langle e| - |g\rangle\langle g|$. $\omega_m(t)$ and $\omega_q(t)$ are time-modulated eigen-frequencies of the bosonic mode and qubit, respectively. The longitudinal interaction $g(t)$ between the transmon qubit and LC oscillator can be tuned by the external flux [74–77], and that between the electron spin and microwave cavity is tunable via the external magnetic field [78–80]. For the bosonic mode with a coherence time $T_2 \sim 1\mu\text{s}$, the longitudinal interaction $g(t)/2\pi$ typically lies in the range [10, 10³]MHz [75, 80]. The Hamiltonian (10) can also be available in the dispersively coupled qubit-bosonic systems, such as cQED systems [38, 81–86] and trapped ion systems [87, 88], by the displacement transformation.

A proper representation is desired to construct the dynamical invariant to generate large-size cat states. We suppose that the relevant unitary transformation $\mathcal{V}(t)$ in Eq. (2) takes a conditional form as

$$\mathcal{V}(t) = D^\dagger[\alpha(t)] \otimes |e\rangle\langle e| + D[\alpha(t)] \otimes |g\rangle\langle g|, \quad (11)$$

where $D[\alpha(t)] \equiv \exp[\alpha(t)m^\dagger - \alpha^*(t)m]$ is a displacement operator with $\alpha(t) = \theta(t)\exp[-i\beta(t)]$. Here $\theta(t)$ and $\beta(t)$ are time-dependent amplitude and phase, respectively.

In the rotating frame with respect to $\mathcal{V}(t)$ in Eq. (11), $H(t)$ in Eq. (10) is transformed as

$$\begin{aligned} H_{\text{rot}}(t) &= \mathcal{V}^\dagger(t)H(t)\mathcal{V}(t) - i\mathcal{V}^\dagger(t)\frac{\partial\mathcal{V}(t)}{\partial t} \\ &= [H_e(t) - \mathcal{A}_e(t)] \otimes |e\rangle\langle e| + [H_g(t) - \mathcal{A}_g(t)] \otimes |g\rangle\langle g|. \end{aligned} \quad (12)$$

Here we have two conditional dynamical components:

$$\begin{aligned} H_{e,g}(t) &= \omega_m m^\dagger m \pm \frac{\omega_q}{2} - \omega_m \theta^2(t) \\ &\pm \left\{ \left[g(t)e^{i\varphi} - \omega_m \theta(t)e^{i\beta(t)} \right] \left[m \mp \theta(t)e^{-i\beta(t)} \right] + \text{H.c.} \right\}, \end{aligned} \quad (13)$$

and two conditional gauge potentials:

$$\begin{aligned} \mathcal{A}_{e,g}(t) &= \pm i \left\{ \partial_t \left[\theta(t)e^{i\beta(t)} \right] \left[m \mp \theta(t)e^{-i\beta(t)} \right] \right. \\ &\quad \left. - \partial_t \left[\theta(t)e^{-i\beta(t)} \right] \left[m^\dagger \mp \theta(t)e^{i\beta(t)} \right] \right\}, \end{aligned} \quad (14)$$

To cancel the linear terms of $H_{\text{rot}}(t)$ in Eq. (12), one can impose constraints on eigenfrequencies, coupling strength, and coupling phase, in Eq. (13), in accordance to the gauge potentials in Eq. (14). Particularly, we have

$$\omega_m(t) = \dot{\beta}(t), \quad g(t) = \dot{\theta}(t), \quad \varphi = \beta(t) + \frac{\pi}{2}. \quad (15)$$

The constraint on the eigenfrequency of the qubit is relaxed. Equation (15) suggests that the systematic parameters in $H(t)$ are not necessarily time-dependent, provided that $\theta(t)$ and $\beta(t)$ can be chosen as a linear function of time and constant, respectively. And using Eq. (15), $H_{\text{rot}}(t)$ in Eq. (12) is reduced to

$$H_{\text{rot}}(t) = \omega_m(t)m^\dagger m + \frac{\omega_q(t)}{2}\sigma_z - \omega_m(t)\theta^2(t). \quad (16)$$

Then according to Eq. (3), the relevant dynamical invariant with a vanishing global phase is found to be

$$\mu(0) = |0\rangle\langle 0| \otimes |e\rangle\langle e| + |0\rangle\langle 0| \otimes |g\rangle\langle g|, \quad (17)$$

where $|0\rangle$ is the vacuum state of the bosonic mode. Using $\mathcal{V}(t)$ in Eq. (11), the evolution of $\mu(0)$ in the original picture can be obtained as

$$\begin{aligned} \mu(t) &= \mathcal{V}(t)\mu(0)\mathcal{V}^\dagger(t) \\ &= |-\alpha(t)\rangle\langle -\alpha(t)| \otimes |e\rangle\langle e| + |\alpha(t)\rangle\langle \alpha(t)| \otimes |g\rangle\langle g|. \end{aligned} \quad (18)$$

This result indicates that when the composite system is initially in the product state $|\Psi(0)\rangle = |0\rangle \otimes |\pm\rangle$ with $|\pm\rangle \equiv (|e\rangle \pm |g\rangle)/\sqrt{2}$, it will become a highly entangled state $|\Psi(\tau)\rangle = (|C_\alpha^+(\tau)\rangle \otimes |\pm\rangle \mp |C_\alpha^-(\tau)\rangle \otimes |\mp\rangle)/\sqrt{2}$ at the desired time τ , where the cat states are defined as $|C_\alpha^\pm(t)\rangle \equiv [|\alpha(t)\rangle \pm |-\alpha(t)\rangle]/\mathcal{N}$ with the normalized coefficient \mathcal{N} . Upon a projective measurement on the qubit basis $|\pm\rangle$ or $|\mp\rangle$, the bosonic mode will be prepared as the cat state $|C_\alpha^+(\tau)\rangle$ or $|C_\alpha^-(\tau)\rangle$.

With no loss of generality, the composite system is assumed to be initialized as a product state $|\psi(0)\rangle = |0\rangle \otimes |+\rangle$. The system wave-function $|\psi(t)\rangle$ is numerically obtained by the time-dependent Schrödinger equation $id|\psi(t)\rangle/dt = H(t)|\psi(t)\rangle$ with the full Hamiltonian in Eq. (10). The protocol performance can be evaluated by the fidelity $\mathcal{F}(t) = |\langle\Psi(\tau)|\psi(t)\rangle|^2$ with the target state $|\Psi(\tau)\rangle = (|C_\alpha^+(\tau)\rangle \otimes |+\rangle - |C_\alpha^-(\tau)\rangle \otimes |-\rangle)/\sqrt{2}$ at the target moment τ and the mean photon number $\bar{n} \equiv \langle\psi(t)|m^\dagger m|\psi(t)\rangle$. On performing a projective measurement on $|+\rangle$, the composite system collapses to the tensor product state of a qubit state $|+\rangle$ and a normalized wave function of the resonator $|\psi_b(t)\rangle = \sqrt{2}\langle +|\psi(t)\rangle$. The latter can be illustrated by the Wigner function in the phase space $W(\alpha) \equiv (2/\pi)\text{Tr}[\rho_b(t)D(\alpha)(-1)^{m^\dagger m}D^\dagger(\alpha)]$ with the bosonic density matrix $\rho_b(t) = |\psi_b(t)\rangle\langle\psi_b(t)|$. Note $\bar{n} = \langle\psi_b(t)|m^\dagger m|\psi_b(t)\rangle$.

Figure 2 demonstrates the Wigner function about the resonator wave-function $|\psi_b(t)\rangle$ at certain moments and the fidelity and mean photon number with respect to various target sizes of the final cat states. More than a precise control over the amplitudes and phases, our protocol enables to demonstrate the large-size cat states with a unit fidelity. In particular, Figs. 2(a)-(c) present the growing size and the rotation in phase space of the resonator states at $t = \tau/4$, $\tau/2$, and τ , which are characterized by the amplitudes and the phases $[\theta, \beta] = (\pi/4, 5\pi/8)$, $(\pi/2, 3\pi/4)$, and (π, π) , respectively. Figure 2(d) confirms the quality of the final highly entangled cat state

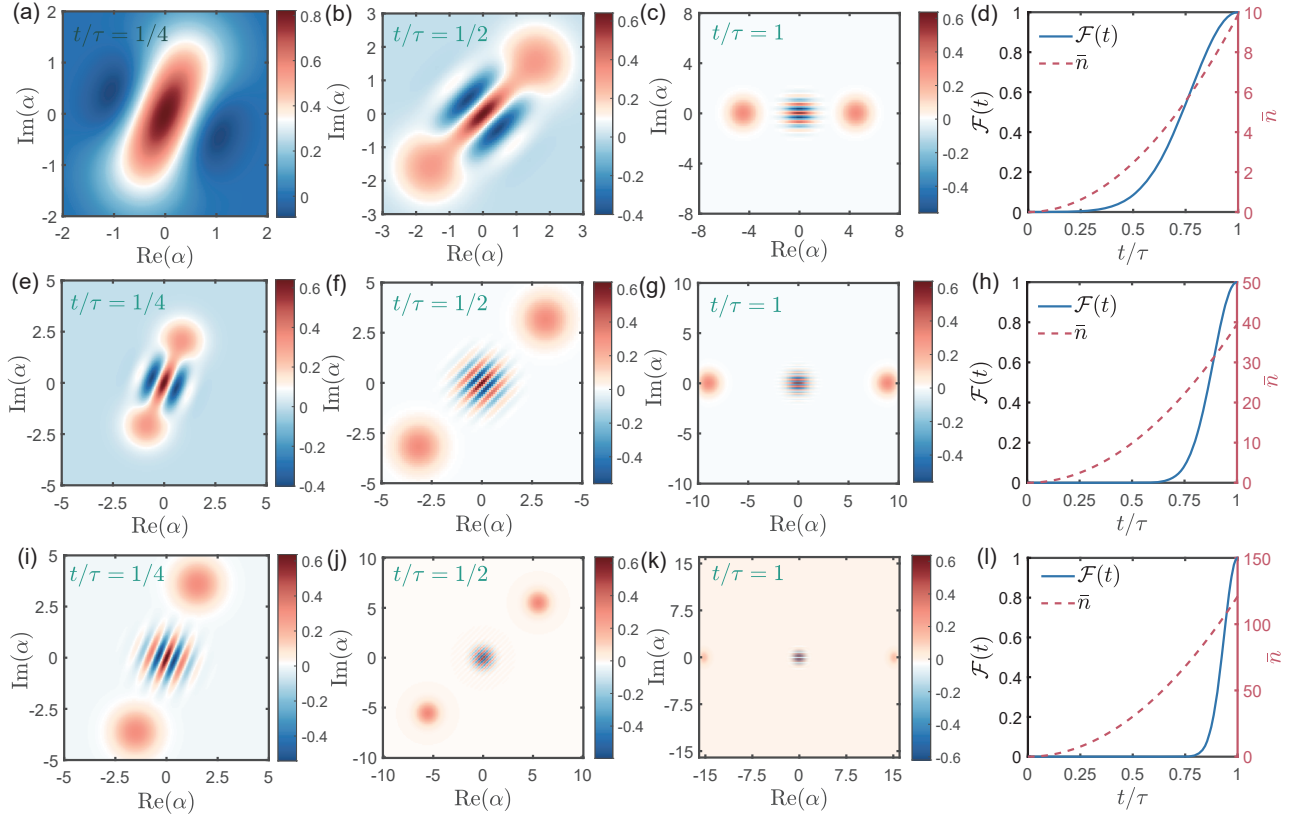


FIG. 2. Wigner functions of specific moments t/τ describing the evolution process of the resonator from vacuum state to cat state. The first three panels of each line, e.g., (a-c), (e-g), and (i-k) are associated with the resonator states $|\psi_b(t)\rangle$ with various amplitudes or $|\alpha|$, obtained by performing projective measurement on the basis $|+\rangle$ of the qubit. The relevant dynamics about the target state fidelity and the mean photon number for the final entangled states $|\Psi(\tau)\rangle = (|C_\alpha^+(\tau)\rangle \otimes |+\rangle - |C_\alpha^-(\tau)\rangle \otimes |-\rangle)/\sqrt{2}$ appears at the rightmost panel of each line, e.g., (d), (h), and (l). The evolution period is set as $\tau \sim 1\mu\text{s}$. The system is initially in the product state $|\psi(0)\rangle = |\Psi(0)\rangle = |0\rangle \otimes |+\rangle$. The eigenfrequency of the bosonic mode $\omega_m(t)$, the longitudinal interaction $g(t)$, and the phase φ are set by Eq. (15) with $\beta(t) = \pi t/(2\tau) + \pi/2$ and in (a-d) $\theta(t) = \pi t/\tau$, in (e-h) $\theta(t) = 2\pi t/\tau$, and in (i-l) $\theta(t) = 7\pi t/2\tau$.

with fidelity $\mathcal{F}(\tau) = 1$ and the mean photon number $\bar{n} \sim 10$ at $t = \tau$. Similarly, the panels of the second line of Fig. 2 present the generation process toward the cat state with amplitude $|\alpha(\tau)| = \theta(\tau) = 2\pi$. As expected, it is verified for a larger-size cat state that the distance between the two peaks in its Wigner function shown in Fig. 2(g) is longer than that in Fig. 2(c). And in the end of the protocol, $t = \tau$, the highly entangled cat state is generated with the mean photon number $\bar{n} \sim 40$ and a unit fidelity, as shown in Fig. 2(h). Comparing the second line to the first line, it is found that the interference pattern becomes clearer with increasing variation rate of $\theta(t)$. The third line of Fig. 2 demonstrates the generation of an ultra-large cat state with amplitude $|\alpha| = \theta > 10$. As shown in Fig. 2(l), the target highly entangled cat state with $\theta(\tau) = 3.5\pi$ is confirmed with $\mathcal{F}(\tau) = 1$ and $\bar{n} \sim 120$.

IV. GENERATION OF CAT STATES IN OPEN QUBIT-BOSONIC SYSTEMS

In this section, our protocol is extended to the open quantum systems for generating the large-amplitude cat states. Consider the open hybrid qubit-bosonic system plotted in Fig. 1, whose dynamics is generally described by the Lindblad master equation but can be effectively described by a non-Hermitian Hamiltonian under partial postselection (see Appendix A for the derivation details). The full non-Hermitian Hamiltonian can be expressed as

$$\begin{aligned}
 H(t) = & \left[\omega_m(t) - i \frac{\gamma_m e^{i\varphi_m}}{2} \right] m^\dagger m \\
 & + \frac{1}{2} \left[\omega_q(t) \sigma_z - \frac{i}{2} (\gamma_e e^{i\varphi_e} |e\rangle\langle e| + \gamma_g e^{i\varphi_g} |g\rangle\langle g|) \right] \\
 & + g(t) \sigma_z (m e^{i\varphi} + m^\dagger e^{-i\varphi}),
 \end{aligned} \tag{19}$$

where $\gamma_m > 0$, $\gamma_e > 0$, and $\gamma_g > 0$ denote the gain or loss rates of the bosonic mode and the levels $|e\rangle$ and $|g\rangle$, respectively, and the effects of the gain or loss depend on

the phases φ_m , φ_e , and φ_g . Without loss of generality, we assume $\gamma_e = \gamma_g = \gamma$, $\varphi_e = \varphi_g = \pi$ and $\varphi_g = \varphi_e + \pi$ as follows. Then the non-Hermitian Hamiltonian (19) is reduced to

$$H(t) = \tilde{\omega}_m(t)m^\dagger m + \frac{\tilde{\omega}_q(t)}{2}\sigma_z + g(t)\sigma_z (me^{i\varphi} + m^\dagger e^{-i\varphi}), \quad (20)$$

with $\tilde{\omega}_m(t) = \omega_m(t) - i\gamma_m \exp(i\varphi_m)/2$ and $\tilde{\omega}_q(t) = \omega_q(t) - i\gamma \exp(i\varphi_q)/2$. If $\varphi_m = \varphi_q = \pi$ or $\varphi_m = \varphi_q = 0$, then the composite system is under gain or loss, respectively.

In the non-Hermitian scenario, the conditional unitary transformation $\mathcal{V}(t)$ in Eq. (11) has to be modified with the displacement amplitudes that embody extra amplification or attenuation. Then we have

$$\tilde{\mathcal{V}}(t) = D^\dagger[\tilde{\alpha}(t)] \otimes |e\rangle\langle e| + D[\tilde{\alpha}(t)] \otimes |g\rangle\langle g|, \quad (21)$$

where the time-dependent displacement operator is defined by $D[\tilde{\alpha}(t)] \equiv \exp[\tilde{\alpha}(t)m^\dagger - \tilde{\alpha}^*(t)m]$ with $\tilde{\alpha}(t) = \theta(t) \exp[-i\beta(t) - \beta_i(t)]$. $\theta(t)$, $\beta(t)$, and $\beta_i(t)$ are time-dependent real parameters. In the rotating frame with respect to $\tilde{\mathcal{V}}(t)$ in Eq. (21), $H(t)$ in Eq. (20) is transformed as

$$\begin{aligned} H_{\text{rot}}(t) &= \tilde{\mathcal{V}}^\dagger(t)H(t)\tilde{\mathcal{V}}(t) - i\tilde{\mathcal{V}}^\dagger(t)\frac{\partial\tilde{\mathcal{V}}(t)}{\partial t} \\ &= [\tilde{H}_e(t) - \tilde{\mathcal{A}}_e(t)] \otimes |e\rangle\langle e| + [\tilde{H}_g(t) - \tilde{\mathcal{A}}_g(t)] \otimes |g\rangle\langle g|, \end{aligned} \quad (22)$$

where the non-Hermitian conditional dynamical components $\tilde{H}_e(t)$ and $\tilde{H}_g(t)$, and the conditional gauge potentials $\tilde{\mathcal{A}}_e$ and $\tilde{\mathcal{A}}_g$, take the similar forms as those in Eqs. (13) and (14), respectively, under the replacements of $\omega_m(t) \rightarrow \tilde{\omega}_m(t)$, $\omega_q(t) \rightarrow \tilde{\omega}_q(t)$, and $\alpha(t) \rightarrow \tilde{\alpha}(t)$.

Using $\tilde{\mathcal{A}}_e$ and $\tilde{\mathcal{A}}_g$, the linear terms of $H_{\text{rot}}(t)$ in Eq. (22) can be neutralized by imposing the following constraints on the dynamical components:

$$\begin{aligned} \omega_m(t) &= \dot{\beta}(t) + \frac{\gamma_m}{2} \sin \varphi_m, & g(t) &= \dot{\theta}(t)e^{-\beta_i(t)}, \\ \varphi &= \beta(t) + \frac{\pi}{2}, & \gamma_m \cos \varphi_m &= -2\dot{\beta}_i(t), \end{aligned} \quad (23)$$

under which, $H_{\text{rot}}(t)$ (22) is simplified as

$$H_{\text{rot}}(t) = \tilde{\omega}_m(t)m^\dagger m + \frac{\tilde{\omega}_q(t)}{2}\sigma_z - \tilde{\omega}_m(t)|\tilde{\alpha}(t)|^2. \quad (24)$$

It is interesting to find that the Heisenberg equation (3) for the dynamical invariant $\mu(0)$ in Eq. (17) for the Hermitian case is capable to yield the dynamical invariant for the non-Hermitian case, when using the non-Hermitian rotated Hamiltonian $H_{\text{rot}}(t)$. By the inversion of $\tilde{\mathcal{V}}(t)$ in Eq. (21), the dynamics of $\mu(0)$ in the original picture is found to be

$$\begin{aligned} \mu(t) &= \tilde{\mathcal{V}}(t)\mu(0)\tilde{\mathcal{V}}^\dagger(t) \\ &= |-\tilde{\alpha}(t)\rangle\langle -\tilde{\alpha}(t)| \otimes |e\rangle\langle e| + |\tilde{\alpha}(t)\rangle\langle \tilde{\alpha}(t)| \otimes |g\rangle\langle g|. \end{aligned} \quad (25)$$

In contrast to the Hermitian result in Eq. (18), now the amplitude of the coherent state is equipped with an extra factor, i.e., $\alpha(t) \rightarrow \tilde{\alpha}(t) = \alpha(t) \exp[-\beta_i(t)]$, which attributes substantially to the non-Hermitian component in Eqs. (19) or (20) and contributes to the probability nonconservation of the system wave-function.

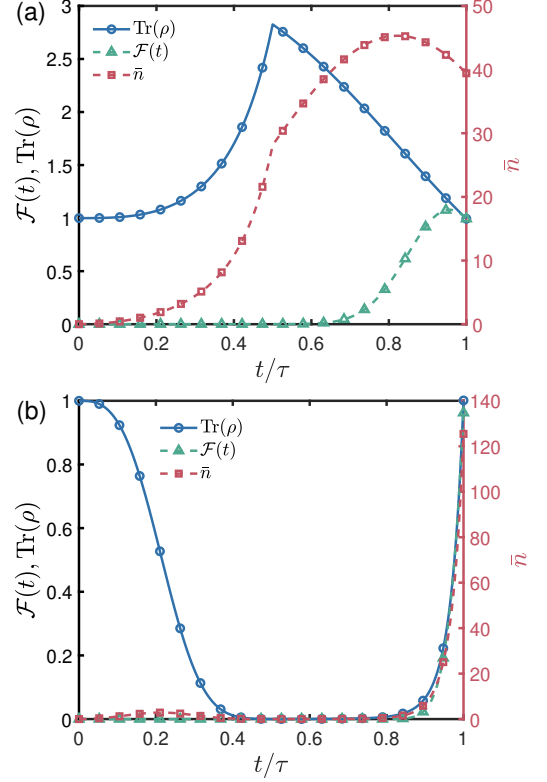


FIG. 3. Dynamics of the density-matrix trace about the whole system $\text{Tr}[\rho(t)]$, the fidelity $\mathcal{F}(t)$ with respect to the target state $|\Psi(\tau)\rangle = (|C_\alpha^+(\tau)\rangle \otimes |+\rangle - |C_\alpha^-(\tau)\rangle \otimes |-\rangle)/\sqrt{2}$, and the mean photon number $\bar{n}(t)$. The evolution period is set as $\tau \sim 1\mu\text{s}$. The system is initially in the product state $|\psi(0)\rangle = |0\rangle \otimes |+\rangle$. The eigenfrequency of the bosonic mode $\omega_m(t)$, the longitudinal coupling strength $g(t)$, the phase φ , and the gain or loss rate of the bosonic mode γ_m are set by Eq. (23) where $\beta(t) = \pi t/(2\tau) + \pi/2$ and $\beta_i(t)$ in Eq. (27) with (a) $\lambda_1 = 1/20$, $\lambda_2 = -0.143\lambda_1$, $\theta(t) = 2\pi t/\tau$ and (b) $\lambda_1 = -1/10$, $\lambda_2 = 0.142\lambda_1$, $\theta(t) = 7\pi t/2\tau$. The longitudinal coupling strength is larger than the gain or loss rates by one order in magnitude. $g/\gamma_m \sim 10$ for $t \in [0, \tau/2]$ and $g/\gamma_m \sim 20$ for $t \in [\tau/2, \tau]$.

To save the probability conservation at the target moment $t = \tau$, the whole evolution can be parameterized to two stages as (i) $t_1 \in [0, \tau/2]$ and (ii) $t_2 \in [\tau/2, \tau]$. During one of them, the bosonic mode is subject to the loss effect and during the other, it is dominated by the gain effect. Due to Eqs. (23) and (25), at the turning point $t = \tau/2$, the sudden switching from the gain effect to loss effect (or vice versa) can be realized by a sudden change in $\beta_i(t)$. Despite the parameters might be non-differentiable, however, the system dynamics presented by the dynamical invariant is required to be con-

tinuous around the vicinity of the tuning point. Thus $\mu(t = \tau^-/2) \approx \mu(t = \tau^+/2)$ gives rise to a criterion:

$$\left\langle -\tilde{\alpha}\left(\frac{\tau^-}{2}\right) \middle| -\tilde{\alpha}\left(\frac{\tau^+}{2}\right) \right\rangle = \left\langle \tilde{\alpha}\left(\frac{\tau^-}{2}\right) \middle| \tilde{\alpha}\left(\frac{\tau^+}{2}\right) \right\rangle \approx 1. \quad (26)$$

According to Eq. (23), the system can undergo a switching between the gain and loss effects in two stages by simply setting $\beta_i(t)$ as

$$\begin{aligned} \beta_i(t) &= \lambda_1 \theta(t), & t \in [0, \tau/2], \\ \beta_i(t) &= \lambda_2 \theta(t), & t \in [\tau/2, \tau], \end{aligned} \quad (27)$$

where the coefficients λ_1 and λ_2 are of opposite signs. Consequently, the criterion in Eq. (26) can be simplified as $|\exp(-\lambda_1 \theta(\tau^-/2)) - \exp(-\lambda_2 \theta(\tau^+/2))|^2 \approx 0$, which is always attainable under appropriate choices of λ_1 and λ_2 . For the composite system initially in the state $|\psi(0)\rangle = |0\rangle \otimes |+\rangle$, it will evolve to a highly entangled cat state at $t = \tau$. The gain or loss rate of the qubit is set as $\gamma\tau = 0.5$ with $\varphi_q = 0$ when $t \in [0, \tau/2]$ and $\varphi_q = \pi$ when $t \in [\tau/2, \tau]$ to automatically normalize $|\psi(\tau)\rangle$.

Figure 3 demonstrates the dynamics of the trace of the density matrix $\text{Tr}[\rho(t)]$ with $\rho(t) = |\psi(t)\rangle\langle\psi(t)|$, the target state fidelity $\mathcal{F}(t)$, and the mean photon number \bar{n} . In Fig. 3(a), the system is subject to gain and loss effects in stages (i) and (ii), respectively, whereas in Fig. 3(b), the stages of gain and loss are reversed. In particular, in Fig. 3(a), the trace first increases to be greater than unit in stage (i) and then decreases in stage (ii). And in Fig. 3(b), the behavior is roughly reversed. In both of them, $\text{Tr}(\rho) \approx 1$ is attained at $t = \tau$. It is found that the target highly entangled cat states with ultralarge amplitudes can be obtained at the final moment. In Fig. 3(a), we have a nearly unit-fidelity target state $\mathcal{F}(\tau) \approx 1$ with the mean photon number $\bar{n} \sim 40$ when $t = \tau$; and in Fig. 3(b), we have a cat state with $\mathcal{F}(\tau) > 0.962$ and $\bar{n} \sim 120$.

V. INTRINSIC CAT STATES AND FOUR-LEGGED CAT STATES

A. Generation of intrinsic cat states

In the context of the Schrödinger's gedanken experiment [1], the cat state is intrinsically a highly entangled state of three components in the whole system, e.g., the dead or live cat, the broken or unbroken poison bottle. The latter two components can be modeled as two individual qubits. Then the intrinsic cat state can be defined as

$$|\mathcal{C}_{\text{int}}\rangle = \frac{1}{\mathcal{N}_a} [|-\alpha\rangle|e\rangle_1|e\rangle_2 + |\alpha\rangle|g\rangle_1|g\rangle_2], \quad (28)$$

where \mathcal{N}_a is the normalization factor and $|e\rangle_j$ and $|g\rangle_j$, $j = 1, 2$, denote the excited and ground states of the

j th qubit. To generate such a three-partite entangled state, we consider an open quantum system [74–81] with a Hamiltonian directly extended from Eq. (19) or (20):

$$\begin{aligned} H(t) &= \tilde{\omega}_m(t)m^\dagger m + \frac{\tilde{\omega}_q(t)}{2} [\sigma_z^{(1)} + \sigma_z^{(2)}] \\ &+ g_1(t)\sigma_z^{(1)} (me^{i\varphi_1} + \text{H.c.}) + g_2(t)\sigma_z^{(2)} (me^{i\varphi_2} + \text{H.c.}). \end{aligned} \quad (29)$$

Under the isotropic conditions of $g_1(t) = g_2(t) = g(t)/2$ and $\varphi_1 = \varphi_2 = \varphi$, the system dynamics under the Hamiltonian (29) can be restricted within the subspace spanned by $|ee\rangle \equiv |e\rangle_1 \otimes |e\rangle_2$ and $|gg\rangle \equiv |g\rangle_1 \otimes |g\rangle_2$. Then we have

$$H(t) = H_e(t) \otimes |ee\rangle\langle ee| + H_g(t) \otimes |gg\rangle\langle gg| \quad (30)$$

with the conditional Hamiltonian

$$H_{e,g}(t) = \tilde{\omega}_m(t)m^\dagger m \pm \tilde{\omega}_q(t) \pm g(t) (me^{i\varphi} + m^\dagger e^{-i\varphi}). \quad (31)$$

The dynamics of the bosonic mode is therefore conditioned on the two-qubit product states, i.e., $|ee\rangle$ and $|gg\rangle$, which is similar to Eq. (20) conditioned by the single-qubit state.

In the rotating frame with respect to the conditional unitary transformation $\tilde{\mathcal{V}}(t)$, obtained by Eq. (21) with the replacements of $|e\rangle \rightarrow |ee\rangle$ and $|g\rangle \rightarrow |gg\rangle$, the transformed Hamiltonian is expressed as

$$\begin{aligned} H_{\text{rot}}(t) &= \tilde{\mathcal{V}}^\dagger(t)H(t)\tilde{\mathcal{V}}(t) - i\tilde{\mathcal{V}}^\dagger(t)\frac{\partial\tilde{\mathcal{V}}(t)}{\partial t} \\ &= [\tilde{H}_e(t) + \frac{\tilde{\omega}_q(t)}{2}] \otimes |ee\rangle\langle ee| \\ &+ [\tilde{H}_g(t) - \frac{\tilde{\omega}_q(t)}{2}] \otimes |gg\rangle\langle gg|. \end{aligned} \quad (32)$$

Here the conditional rotated Hamiltonian $\tilde{H}_e(t)$ and $\tilde{H}_g(t)$ share the same expression of their counterparts in Eq. (22). Again, under the parametric constraints in Eq. (23), the transformed Hamiltonian $H_{\text{rot}}(t)$ can be reduced to

$$\begin{aligned} H_{\text{rot}}(t) &= \tilde{\omega}_m(t)m^\dagger m (|ee\rangle\langle ee| + |gg\rangle\langle gg|) \\ &+ \tilde{\omega}_q(t)(|ee\rangle\langle ee| - |gg\rangle\langle gg|) - \tilde{\omega}_m(t)|\tilde{\alpha}(t)|^2, \end{aligned} \quad (33)$$

which satisfies the Heisenberg equation (3) with the stationary dynamical invariant

$$\mu(0) = |0\rangle\langle 0| \otimes |ee\rangle\langle ee| + |0\rangle\langle 0| \otimes |gg\rangle\langle gg|. \quad (34)$$

By the inversion of $\tilde{\mathcal{V}}(t)$, the time evolution of $\mu(0)$ in the original picture is found to be similar to Eq. (25):

$$\begin{aligned} \mu(t) &= \tilde{\mathcal{V}}(t)\mu(0)\tilde{\mathcal{V}}^\dagger(t) \\ &= |-\tilde{\alpha}(t)\rangle\langle -\tilde{\alpha}(t)| \otimes |ee\rangle\langle ee| + |\tilde{\alpha}(t)\rangle\langle \tilde{\alpha}(t)| \otimes |gg\rangle\langle gg|. \end{aligned} \quad (35)$$

Consequently, the criterion in Eq. (26) still guarantees the norm conservation of the wave function at the target moment τ . Starting from the initial state $|\Psi(0)\rangle =$

$|0\rangle \otimes (|ee\rangle + |gg\rangle)/\sqrt{2}$ (Note that it is consistent with the correlation between the radioactive atom and the poison bottle assumed by Schrödinger), the system will approach the intrinsic cat state $|\Psi(\tau)\rangle = (|-\alpha(\tau)\rangle|ee\rangle + |\alpha(\tau)\rangle|gg\rangle)/\sqrt{2}$. When the parameters in Hamiltonian in Eq. (30) are of the comparable order in magnitude to those in Fig. 3(b), one can also verify that the intrinsic cat states can be generated with a close-to-unit fidelity and over 100 in the mean photon number.

B. Generation of four-legged cat states

Based on the hybrid qubit-bosonic system governed by Eq. (29), our protocol can be further extended to the generation of the large-amplitude four-legged cat states, i.e., $|\alpha(t)\rangle + |-\alpha(t)\rangle + |i\alpha(t)\rangle + |-i\alpha(t)\rangle$. To make the bosonic mode in a superposition of coherent states with four distinct phases, we assume that the coupling strengths are $g_1(t) = g_2(t) = g(t)/\sqrt{2}$ and the phases are $\varphi_1 = \varphi + \pi/4$ and $\varphi_2 = \varphi + 3\pi/4$ with the phase φ subject to Eq. (23), then the non-Hermitian Hamiltonian (29) is transformed as

$$\begin{aligned} H(t) &= \tilde{\omega}_m(t)m^\dagger m + \frac{\tilde{\omega}_q(t)}{2}[\sigma_z^{(1)} + \sigma_z^{(2)}] \\ &+ ig(t)(|ee\rangle\langle ee| - |gg\rangle\langle gg|)(me^{i\varphi} - m^\dagger e^{-i\varphi}) \\ &+ g(t)(|eg\rangle\langle eg| - |ge\rangle\langle ge|)(me^{i\varphi} + m^\dagger e^{-i\varphi}). \end{aligned} \quad (36)$$

Similar to Eq. (21), the conditional unitary transformation $\tilde{\mathcal{V}}(t)$ for the generation of four-legged cat states takes the form of

$$\begin{aligned} \tilde{\mathcal{V}}(t) &= D^\dagger[-\tilde{\alpha}(t)] \otimes |ee\rangle\langle ee| + D[\tilde{\alpha}(t)] \otimes |gg\rangle\langle gg| \\ &+ D^\dagger[-i\tilde{\alpha}(t)] \otimes |eg\rangle\langle eg| + D[i\tilde{\alpha}(t)] \otimes |ge\rangle\langle ge|. \end{aligned} \quad (37)$$

Then in the rotating frame with respect to $\tilde{\mathcal{V}}(t)$, $H(t)$ in Eq. (36) is transformed as

$$\begin{aligned} H_{\text{rot}}(t) &= \tilde{\mathcal{V}}^\dagger(t)H(t)\tilde{\mathcal{V}}(t) - i\tilde{\mathcal{V}}^\dagger(t)\frac{\partial\tilde{\mathcal{V}}(t)}{\partial t} \\ &= \tilde{\mathcal{H}}_e(t) \otimes |ee\rangle\langle ee| + \tilde{\mathcal{H}}_g(t) \otimes |gg\rangle\langle gg| \\ &+ \tilde{\mathcal{H}}_e^i(t) \otimes |eg\rangle\langle eg| + \tilde{\mathcal{H}}_g^i(t) \otimes |ge\rangle\langle ge|, \end{aligned} \quad (38)$$

where the conditional rotated Hamiltonian $\tilde{\mathcal{H}}_e(t)$ and $\tilde{\mathcal{H}}_g(t)$ are the same as those in Eq. (22), and $\tilde{\mathcal{H}}_e^i(t)$ and $\tilde{\mathcal{H}}_g^i(t)$ take the similar forms as $\tilde{\mathcal{H}}_e(t)$ and $\tilde{\mathcal{H}}_g(t)$, respectively, with the replacement of $\tilde{\alpha}(t) \rightarrow i\tilde{\alpha}(t)$.

The linear terms of $H_{\text{rot}}(t)$ in Eq. (38) can be canceled by the constraints in Eq. (23). And then we have

$$\begin{aligned} H_{\text{rot}}(t) &= \tilde{\omega}_m(t)m^\dagger m + \frac{\tilde{\omega}_q(t)}{2}(|ee\rangle\langle ee| - |gg\rangle\langle gg| \\ &+ |eg\rangle\langle eg| - |ge\rangle\langle ge|) - \tilde{\omega}_m(t)|\tilde{\alpha}(t)|^2. \end{aligned} \quad (39)$$

For this Hamiltonian, the dynamical invariant satisfying the Heisenberg equation (3) is found to be

$$\begin{aligned} \mu(0) &= |0\rangle\langle 0| \otimes |ee\rangle\langle ee| + |0\rangle\langle 0| \otimes |gg\rangle\langle gg| \\ &+ |0\rangle\langle 0| \otimes |eg\rangle\langle eg| + |0\rangle\langle 0| \otimes |ge\rangle\langle ge|. \end{aligned} \quad (40)$$

And in the original picture it evolves as

$$\begin{aligned} \mu(t) &= \tilde{\mathcal{V}}(t)\mu(0)\tilde{\mathcal{V}}^\dagger(t) = |-\tilde{\alpha}(t)\rangle\langle -\tilde{\alpha}(t)| \otimes |ee\rangle\langle ee| \\ &+ |\tilde{\alpha}(t)\rangle\langle \tilde{\alpha}(t)| \otimes |gg\rangle\langle gg| + |-i\tilde{\alpha}(t)\rangle\langle -i\tilde{\alpha}(t)| \otimes |eg\rangle\langle eg| \\ &+ |i\tilde{\alpha}(t)\rangle\langle i\tilde{\alpha}(t)| \otimes |ge\rangle\langle ge|. \end{aligned} \quad (41)$$

under the inversion of $\mathcal{V}(t)$ in Eq. (37).

Similar to the two-legged cat state generation, under the continuous condition for the dynamical invariant around the vicinity of the tuning point between the gain and loss stages, i.e., $\mu(t = \tau^-/2) \approx \mu(t = \tau^+/2)$, Eq. (41) gives rise to both Eq. (26) and $\langle -i\tilde{\alpha}(\tau^-/2)| - i\tilde{\alpha}(\tau^+/2)\rangle = \langle i\tilde{\alpha}(\tau^-/2)|i\tilde{\alpha}(\tau^+/2)\rangle \approx 1$. The two criteria are found to be equivalent to each other and they guarantee the norm conservation of the wavefunction of the composite system at the target moment τ .

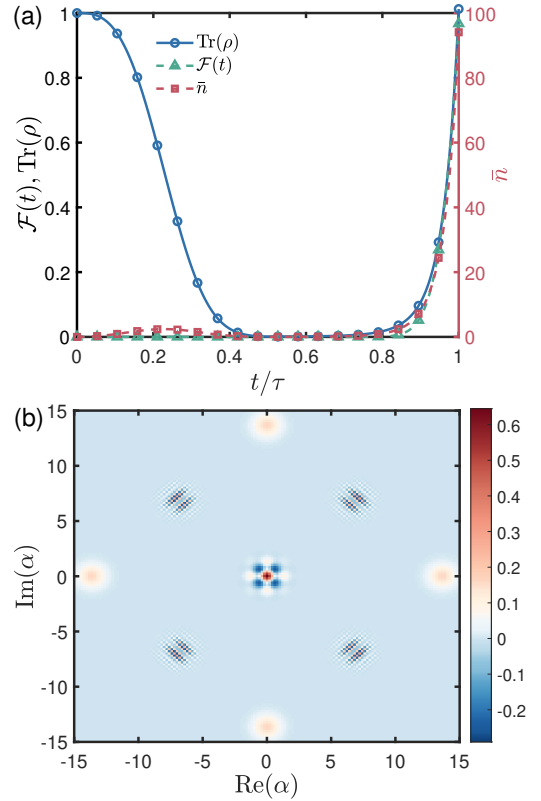


FIG. 4. (a) Dynamics of the density-matrix trace of $\text{Tr}(\rho)$, the target state fidelity $\mathcal{F}(t)$, and the mean photon number \bar{n} of the final entangled state $|\Psi(\tau)\rangle$ in Eq. (42), and (b) Wigner function for the relevant four-legged cat state $|\psi_b(\tau)\rangle = |C_\alpha^+(\tau)\rangle + |C_{i\alpha}^+(\tau)\rangle$ at $t = \tau$, obtained by a projective measurement on $|+\rangle_1|+\rangle_2$ of the composite system. The parameters are set the same as Fig. 3(b) except $\theta(t) = 3\pi t/\tau$.

By the dynamical invariant in Eq. (41), the system initially in the product state $|\Psi(0)\rangle = |0\rangle|+\rangle_1|+\rangle_2$ will

evolve to the highly entangled cat state as

$$\begin{aligned} |\Psi(\tau)\rangle &= \frac{1}{2} [|\alpha\rangle|ee\rangle + |i\alpha\rangle|eg\rangle + |-i\alpha\rangle|ge\rangle + |-\alpha\rangle|gg\rangle] \\ &= \frac{1}{2} \left(|\mathcal{C}_{++}\rangle|+\rangle_1|+\rangle_2 + |\mathcal{C}_{-+}\rangle|-\rangle_1|+\rangle_2 \right. \\ &\quad \left. + |\mathcal{C}_{+-}\rangle|+\rangle_1|-\rangle_2 + |\mathcal{C}_{--}\rangle|-\rangle_1|-\rangle_2 \right), \end{aligned} \quad (42)$$

where the four-legged cat states are defined as

$$\begin{aligned} |\mathcal{C}_{++}\rangle &= |\mathcal{C}_\alpha^+(t)\rangle + |\mathcal{C}_{i\alpha}^+(t)\rangle, & |\mathcal{C}_{-+}\rangle &= |\mathcal{C}_\alpha^-(t)\rangle + |\mathcal{C}_{i\alpha}^-(t)\rangle, \\ |\mathcal{C}_{+-}\rangle &= |\mathcal{C}_\alpha^-(t)\rangle - |\mathcal{C}_{i\alpha}^-(t)\rangle, & |\mathcal{C}_{--}\rangle &= |\mathcal{C}_\alpha^+(t)\rangle - |\mathcal{C}_{i\alpha}^+(t)\rangle, \end{aligned} \quad (43)$$

with $|\mathcal{C}_{i\alpha}^\pm(t)\rangle = (|i\alpha(t)\rangle \pm |-\alpha(t)\rangle)/\mathcal{N}$. As an example, after performing the projective measurement on the basis $|+\rangle_1|+\rangle_2$ of two qubits, we have a four-component bosonic cat state $|\mathcal{C}_{++}\rangle$ with a success probability of 25%.

Figure 4(a) demonstrates the dynamics about the trace of the density matrix $\text{Tr}(\rho)$, the target state fidelity $\mathcal{F}(t)$ with respect to the highly entangled cat state $|\Psi(\tau)\rangle$ in Eq. (42) with $|\alpha(\tau)| = 3\pi$, and the mean photon number \bar{n} . It is found that when $t = \tau$, $\text{Tr}(\rho) \sim 1$, $\mathcal{F}(t) > 0.965$, and $\bar{n} \sim 95$. The relevant Wigner function is presented in Fig. 4(b) for the four-component cat state $|\psi_b(\tau)\rangle = |\mathcal{C}_\alpha^+(\tau)\rangle + |\mathcal{C}_{i\alpha}^+(\tau)\rangle$, obtained by performing a projective measurement on the composite system state $|\psi(\tau)\rangle$. The four peaks and their mutual interference confirm the generated four coherent-state components.

VI. CONCLUSION

In summary, we establish a dynamical-invariant-based control protocol for the time-dependent hybrid qubit-bosonic systems, both Hermitian and non-Hermitian, to deterministically generate large-amplitude Schrödinger cat states, intrinsic cat states, and four-legged cat states. The bosonic mode is longitudinally coupled to the ancillary qubit(s). The model can be directly realized or indirectly implemented in dispersively coupled qubit-bosonic systems via displacement operations across various experimental platforms. The basic idea of our protocol is inherited from our universal quantum control theory. In particular, we first describe the system dynamics in the ancillary picture via an unitary transformation associated with the coherent-state basis conditioned on the qubit state, then find a stationary dynamical invariant satisfying the Heisenberg equation with the rotated Hamiltonian, that constrains the systematic parameters, and eventually, the evolution of the dynamical invariant can be determined in the original picture, that yields the controllable and desired system dynamics.

For open quantum systems, the non-Hermitian Hamiltonian can be derived from the Lindblad master equation under the postselection on qubit, and then UQC gives rise to the constraints associated with the gain or loss rates of the system, for activating the dynamical invariant. The system evolution can be divided into two stages

to guarantee the probability preservation at the target moment. For both Hermitian and non-Hermitian systems, our protocol enables to deterministically generate the Schrödinger cat states of three kinds, with a high fidelity and an ultra-large mean photon number. Our work paves a significant path toward the macroscopic quantum states via dynamical invariants.

ACKNOWLEDGMENTS

We acknowledge grant support from the National Natural Science Foundation of China (Grant No. U25A20199) and the ‘‘Pioneer’’ and ‘‘Leading Goose’’ R&D of Zhejiang Province (Grant No. 2025C01028).

Appendix A: Derivation from Lindblad master equation to non-Hermitian Hamiltonian

This appendix provides a detailed derivation of the non-Hermitian Hamiltonian (19) from the Lindblad master equation for a hybrid spin-bosonic system. While the quantum-jump terms for the qubit component are neglected after postselection [70], those for the bosonic mode are fully retained [71, 72]. In general, the dynamics of an open hybrid system consisting of a qubit longitudinally coupled to a bosonic mode can be described by

$$\frac{d}{dt}\rho = -i[H_{\text{coh}}, \rho] + \gamma\mathcal{L}[\sigma_-]\rho + \frac{\gamma_m}{2}\mathcal{L}[m]\rho, \quad (\text{A1})$$

where $H_{\text{coh}} = \omega_m m^\dagger m + (\omega_q/2)\sigma_z + g\sigma_z[m \exp(i\varphi) + m^\dagger \exp(-i\varphi)]$ represents the eigen-energies of the qubit and the bosonic mode and the coherent interaction between them. The Lindblad superoperators are defined as $\mathcal{L}[o]\rho = o\rho o^\dagger - \{o^\dagger o, \rho\}/2$ with $o = \sigma_-, m$. The first and the second superoperators are associated with the individual dissipations of the qubit and the bosonic mode, with the damping rates γ and $\gamma_m/2$, respectively.

Under Eq. (A1), an arbitrary Schrödinger-picture operator \mathcal{O}_S can be connected with the Heisenberg-picture operator $\mathcal{O}_H(t)$ through

$$\begin{aligned} &\text{Tr}[\mathcal{O}_S \dot{\rho}(t)] \\ &= \text{Tr} \left[\mathcal{O}_S \left(-i[H_{\text{coh}}, \rho] + \gamma\mathcal{L}[\sigma_-]\rho + \frac{\gamma_m}{2}\mathcal{L}[m]\rho \right) \right] \\ &= \text{Tr} \left[\left(i[H_{\text{coh}}, \mathcal{O}_S] + \gamma\mathcal{L}^\dagger[\sigma_-]\mathcal{O}_S + \frac{\gamma_m}{2}\mathcal{L}^\dagger[m]\mathcal{O}_S \right) \rho \right] \\ &= \text{Tr} \left[\dot{\mathcal{O}}_H(t) \rho(0) \right], \end{aligned} \quad (\text{A2})$$

where the Hermitian conjugate superoperator is defined as $\mathcal{L}^\dagger[o]\mathcal{O}_S \equiv o^\dagger \mathcal{O}_S o - \{o^\dagger o, \mathcal{O}_S\}/2$. The derivation from the second line to the third one in Eq. (A2) has used the cyclic property of the trace. Thus, the time derivative of $\mathcal{O}_H(t)$ can be expressed by the adjoint Lindblad master

equation as

$$\frac{d}{dt}\mathcal{O}_H(t) = i[H_{\text{coh}}, \mathcal{O}_S] + \gamma\mathcal{L}^\dagger[\sigma_-]\mathcal{O}_S + \frac{\gamma_m}{2}\mathcal{L}^\dagger[m]\mathcal{O}_S. \quad (\text{A3})$$

Using Eq. (A3) and neglecting the quantum jump terms about the qubit, the dynamics of the operators

σ_- and m can be obtained as

$$\begin{aligned} \frac{d}{dt}\sigma_-(t) &= -i\omega_q\sigma_- - \frac{1}{2}\gamma\sigma_- - i2g\sigma_-(me^{i\varphi} + m^\dagger e^{-i\varphi}), \\ \frac{d}{dt}m(t) &= -i\omega_m m - \gamma_m m - i g e^{-i\varphi}\sigma_z. \end{aligned} \quad (\text{A4})$$

The system dynamics described by Eq. (A4) is equivalent to that governed by the Hamiltonian (19) with $\varphi_m = \varphi_e - \pi = \varphi_q = 0$ and $\gamma_e = \gamma_q = \gamma$.

-
- [1] E. Schrödinger, *Die gegenwärtige situation in der quantenmechanik*, *Naturwissenschaften* **23**, 844 (1935).
- [2] F. Fröwis, P. Sekatski, W. Dür, N. Gisin, and N. Sangouard, *Macroscopic quantum states: Measures, fragility, and implementations*, *Rev. Mod. Phys.* **90**, 025004 (2018).
- [3] D. J. Wineland, *Nobel lecture: Superposition, entanglement, and raising schrödinger's cat*, *Rev. Mod. Phys.* **85**, 1103 (2013).
- [4] S. Haroche, *Nobel lecture: Controlling photons in a box and exploring the quantum to classical boundary*, *Rev. Mod. Phys.* **85**, 1083 (2013).
- [5] M. Arndt and K. Hornberger, *Testing the limits of quantum mechanical superpositions*, *Nat. Phys.* **10**, 271 (2014).
- [6] G. S. Agarwal, R. R. Puri, and R. P. Singh, *Atomic schrödinger cat states*, *Phys. Rev. A* **56**, 2249 (1997).
- [7] A. Omran, H. Levine, A. Keesling, G. Semeghini, T. T. Wang, S. Ebadi, H. Bernien, A. S. Zibrov, H. Pichler, S. Choi, J. Cui, M. Rossignolo, P. Rembold, S. Montangero, T. Calarco, M. Endres, M. Greiner, V. Vuletić, and M. D. Lukin, *Generation and manipulation of schrödinger cat states in rydberg atom arrays*, *Science* **365**, 570 (2019).
- [8] C. Song, K. Xu, H. Li, Y.-R. Zhang, X. Zhang, W. Liu, Q. Guo, Z. Wang, W. Ren, J. Hao, H. Feng, H. Fan, D. Zheng, D.-W. Wang, H. Wang, and S.-Y. Zhu, *Generation of multicomponent atomic schrödinger cat states of up to 20 qubits*, *Science* **365**, 574 (2019).
- [9] Y. A. Yang, W.-T. Luo, J.-L. Zhang, S.-Z. Wang, C.-L. Zou, T. Xia, and Z.-T. Lu, *Minute-scale schrödinger-cat state of spin-5/2 atoms*, *Nat. Photon.* **19**, 89 (2025).
- [10] W. Schleich, M. Pernigo, and F. L. Kien, *Nonclassical state from two pseudoclassical states*, *Phys. Rev. A* **44**, 2172 (1991).
- [11] C. C. Gerry and P. L. Knight, *Quantum superpositions and schrödinger cat states in quantum optics*, *Am. J. Phys.* **65**, 964 (1997).
- [12] U. Leonhardt and H. Paul, *Measuring the quantum state of light*, *Prog. Quantum Electron.* **19**, 89 (1995).
- [13] A. J. Leggett, *Testing the limits of quantum mechanics: motivation, state of play, prospects*, *J. Phys.: Condens. Matter* **14**, R415 (2002).
- [14] M. Bild, M. Fadel, Y. Yang, U. von Lüpke, P. Martin, A. Bruno, and Y. Chu, *Schrödinger cat states of a 16-microgram mechanical oscillator*, *Science* **380**, 274 (2023).
- [15] J. B. Brask, I. Rigas, E. S. Polzik, U. L. Andersen, and A. S. Sørensen, *Hybrid long-distance entanglement distribution protocol*, *Phys. Rev. Lett.* **105**, 160501 (2010).
- [16] S.-W. Lee and H. Jeong, *Near-deterministic quantum teleportation and resource-efficient quantum computation using linear optics and hybrid qubits*, *Phys. Rev. A* **87**, 022326 (2013).
- [17] A. Gilchrist, K. Nemoto, W. J. Munro, T. C. Ralph, S. Glancy, S. L. Braunstein, and G. J. Milburn, *Schrödinger cats and their power for quantum information processing*, *J. Opt. B: Quantum Semiclass. Opt.* **6**, S828 (2004).
- [18] J. Joo, W. J. Munro, and T. P. Spiller, *Quantum metrology with entangled coherent states*, *Phys. Rev. Lett.* **107**, 083601 (2011).
- [19] V. Giovannetti, S. Lloyd, and L. Maccone, *Advances in quantum metrology*, *Nat. Photon.* **5**, 222 (2011).
- [20] L. Pezzè, A. Smerzi, M. K. Oberthaler, R. Schmied, and P. Treutlein, *Quantum metrology with nonclassical states of atomic ensembles*, *Rev. Mod. Phys.* **90**, 035005 (2018).
- [21] P. T. Cochrane, G. J. Milburn, and W. J. Munro, *Macroscopically distinct quantum-superposition states as a bosonic code for amplitude damping*, *Phys. Rev. A* **59**, 2631 (1999).
- [22] T. C. Ralph, A. Gilchrist, G. J. Milburn, W. J. Munro, and S. Glancy, *Quantum computation with optical coherent states*, *Phys. Rev. A* **68**, 042319 (2003).
- [23] A. P. Lund, T. C. Ralph, and H. L. Haselgrove, *Fault-tolerant linear optical quantum computing with small-amplitude coherent states*, *Phys. Rev. Lett.* **100**, 030503 (2008).
- [24] M. Mirrahimi, Z. Leghtas, V. V. Albert, S. Touzard, R. J. Schoelkopf, L. Jiang, and M. H. Devoret, *Dynamically protected cat-qubits: a new paradigm for universal quantum computation*, *New J. Phys.* **16**, 045014 (2014).
- [25] A. Grimm, N. E. Frattini, S. Puri, S. O. Mundhada, S. Touzard, M. Mirrahimi, S. M. Girvin, S. Shankar, and M. H. Devoret, *Stabilization and operation of a kerr-cat qubit*, *Nature* **584**, 205 (2020).
- [26] C. Chamberland, K. Noh, P. Arrangoiz-Arriola, E. T. Campbell, C. T. Hann, J. Iverson, H. Putterman, T. C. Bohdanowicz, S. T. Flammia, A. Keller, G. Refael, J. Preskill, L. Jiang, A. H. Safavi-Naeini, O. Painter, and F. G. Brandão, *Building a fault-tolerant quantum computer using concatenated cat codes*, *PRX Quantum* **3**, 010329 (2022).
- [27] J. Hastrup and U. L. Andersen, *All-optical cat-code quantum error correction*, *Phys. Rev. Res.* **4**, 043065 (2022).
- [28] H. Putterman, K. Noh, R. N. Patel, G. A. Peairs, G. S. MacCabe, M. Lee, S. Aghaieimodi, C. T.

- Hann, I. Jarrige, G. Marcaud, Y. He, H. Moradinejad, J. C. Owens, T. Scaffidi, P. Arrangoiz-Arriola, J. Iverson, H. Levine, F. G. S. L. Brandão, M. H. Matheny, and O. Painter, *Preserving phase coherence and linearity in cat qubits with exponential bit-flip suppression*, *Phys. Rev. X* **15**, 011070 (2025).
- [29] R. Lescanne, M. Villiers, T. Peronnin, A. Sarlette, M. Delbecq, B. Huard, T. Kontos, M. Mirrahimi, and Z. Leghtas, *Exponential suppression of bit-flips in a qubit encoded in an oscillator*, *Nat. Phys.* **16**, 509 (2020).
- [30] C. Monroe, D. M. Meekhof, B. E. King, and D. J. Wineland, *A “schrodinger cat” superposition state of an atom*, *Science* **272**, 1131 (1996).
- [31] P. C. Haljan, K.-A. Brickman, L. Deslauriers, P. J. Lee, and C. Monroe, *Spin-dependent forces on trapped ions for phase-stable quantum gates and entangled states of spin and motion*, *Phys. Rev. Lett.* **94**, 153602 (2005).
- [32] M. J. McDonnell, J. P. Home, D. M. Lucas, G. Imreh, B. C. Keitch, D. J. Szwer, N. R. Thomas, S. C. Webster, D. N. Stacey, and A. M. Steane, *Long-lived mesoscopic entanglement outside the lamb-dicke regime*, *Phys. Rev. Lett.* **98**, 063603 (2007).
- [33] H.-Y. Lo, D. Kienzler, L. de Clercq, M. Marinelli, V. Negnevitsky, B. C. Keitch, and J. P. Home, *Spin-motion entanglement and state diagnosis with squeezed oscillator wavepackets*, *Nature* **521**, 336 (2015).
- [34] K. G. Johnson, J. D. Wong-Campos, B. Neyenhuis, J. Mizrahi, and C. Monroe, *Ultrafast creation of large schrodinger cat states of an atom*, *Nat. Commun.* **8**, 697 (2017).
- [35] I. Rojtkov, M. Simoni, E. Zapusek, F. Reiter, and J. Home, *Stabilization of cat-state manifolds using nonlinear reservoir engineering*, *Phys. Rev. X* **16**, 011056 (2026).
- [36] J. E. Mooij, T. P. Orlando, L. Levitov, L. Tian, C. H. van der Wal, and S. Lloyd, *Josephson persistent-current qubit*, *Science* **285**, 1036 (1999).
- [37] J. R. Friedman, V. Patel, W. Chen, S. K. Tolpygo, and J. E. Lukens, *Quantum superposition of distinct macroscopic states*, *Nature* **406**, 43 (2000).
- [38] B. Vlastakis, G. Kirchmair, Z. Leghtas, S. E. Nigg, L. Frunzio, S. M. Girvin, M. Mirrahimi, M. H. Devoret, and R. J. Schoelkopf, *Deterministically encoding quantum information using 100-photon schrodinger cat states*, *Science* **342**, 607 (2013).
- [39] D. V. Sychev, A. E. Ulanov, A. A. Pushkina, M. W. Richards, I. A. Fedorov, and A. I. Lvovsky, *Enlargement of optical schrodinger’s cat states*, *Nat. Photon.* **11**, 379 (2017).
- [40] W. H. Zurek, *Sub-planck structure in phase space and its relevance for quantum decoherence*, *Nature* **412**, 712 (2001).
- [41] Z. Leghtas, G. Kirchmair, B. Vlastakis, M. H. Devoret, R. J. Schoelkopf, and M. Mirrahimi, *Deterministic protocol for mapping a qubit to coherent state superpositions in a cavity*, *Phys. Rev. A* **87**, 042315 (2013).
- [42] Z. Leghtas, G. Kirchmair, B. Vlastakis, R. J. Schoelkopf, M. H. Devoret, and M. Mirrahimi, *Hardware-efficient autonomous quantum memory protection*, *Phys. Rev. Lett.* **111**, 120501 (2013).
- [43] S.-Y. Lee, C.-W. Lee, H. Nha, and D. Kaszlikowski, *Quantum phase estimation using a multi-headed cat state*, *J. Opt. Soc. Am. B* **32**, 1186 (2015).
- [44] P. Zheng, Y. Cai, B. Xu, S. Wen, L. Zhang, Z. Ni, J. Mai, Y. Zeng, L. Lin, L. Hu, X. Deng, S. Liu, J. Shu, Y. Xu, and D. Yu, *Quantum-enhanced dark matter search using cat states*, *Phys. Rev. Lett.* **136**, 171002 (2026).
- [45] S. He, Z.-L. Yang, S. Jin, F.-Y. Zhang, and C. Li, *Generation of four-component magnonic schrodinger cat states via floquet engineering*, *Phys. Rev. A* **113**, 013739 (2026).
- [46] Z.-J. Chen, W. Cai, L.-X. Xie, Q.-X. Jie, X.-B. Zou, G.-C. Guo, L. Sun, and C.-L. Zou, *Fault-tolerant preparation of arbitrary logical states in the cat code*, *arXiv:2602.17438* (2026).
- [47] J. I. Cirac, M. Lewenstein, K. Mølmer, and P. Zoller, *Quantum superposition states of bose-einstein condensates*, *Phys. Rev. A* **57**, 1208 (1998).
- [48] H. Goto, *Universal quantum computation with a nonlinear oscillator network*, *Phys. Rev. A* **93**, 050301(R) (2016).
- [49] S. Puri, S. Boutin, and A. Blais, *Engineering the quantum states of light in a kerr-nonlinear resonator by two-photon driving*, *npj Quantum Inf.* **3**, 18 (2017).
- [50] T. Hatomura, *Shortcuts to adiabatic cat-state generation in bosonic josephson junctions*, *New J. Phys.* **20**, 015010 (2018).
- [51] D. Iyama, T. Kamiya, S. Fujii, H. Mukai, Y. Zhou, T. Nagase, A. Tomonaga, R. Wang, J.-J. Xue, S. Watabe, S. Kwon, and J.-S. Tsai, *Observation and manipulation of quantum interference in a superconducting kerr parametric oscillator*, *Nat. Commun.* **15**, 86 (2023).
- [52] Y.-H. Chen, W. Qin, X. Wang, A. Miranowicz, and F. Nori, *Shortcuts to adiabaticity for the quantum rabi model: Efficient generation of giant entangled cat states via parametric amplification*, *Phys. Rev. Lett.* **126**, 023602 (2021).
- [53] B. Hacker, S. Welte, S. Daiss, A. Shaikat, S. Ritter, L. Li, and G. Rempe, *Deterministic creation of entangled atom-light schrodinger-cat states*, *Nat. Photon.* **13**, 110 (2019).
- [54] A. P. Lund, H. Jeong, T. C. Ralph, and M. S. Kim, *Conditional production of superpositions of coherent states with inefficient photon detection*, *Phys. Rev. A* **70**, 020101(R) (2004).
- [55] J. S. Neergaard-Nielsen, B. M. Nielsen, C. Hettich, K. Mølmer, and E. S. Polzik, *Generation of a superposition of odd photon number states for quantum information networks*, *Phys. Rev. Lett.* **97**, 083604 (2006).
- [56] T. Gerrits, S. Glancy, T. S. Clement, B. Calkins, A. E. Lita, A. J. Miller, A. L. Migdall, S. W. Nam, R. P. Mirin, and E. Knill, *Generation of optical coherent-state superpositions by number-resolved photon subtraction from the squeezed vacuum*, *Phys. Rev. A* **82**, 031802(R) (2010).
- [57] A. Laghaout, J. S. Neergaard-Nielsen, I. Rigas, C. Kragh, A. Tipsmark, and U. L. Andersen, *Amplification of realistic schrodinger-cat-state-like states by homodyne heralding*, *Phys. Rev. A* **87**, 043826 (2013).
- [58] K. Takase, J.-i. Yoshikawa, W. Asavanant, M. Endo, and A. Furusawa, *Generation of optical schrodinger cat states by generalized photon subtraction*, *Phys. Rev. A* **103**, 013710 (2021).
- [59] F.-X. Sun, S.-S. Zheng, Y. Xiao, Q. Gong, Q. He, and K. Xia, *Remote generation of magnon schrodinger cat state via magnon-photon entanglement*, *Phys. Rev. Lett.* **127**, 087203 (2021).
- [60] L. Gilles, B. M. Garraway, and P. L. Knight, *Generation of nonclassical light by dissipative two-photon processes*,

Phys. Rev. A **49**, 2785 (1994).

- [61] Z. Leghtas, S. Touzard, I. M. Pop, A. Kou, B. Vlastakis, A. Petrenko, K. M. Sliwa, A. Narla, S. Shankar, M. J. Hatridge, M. Reagor, L. Frunzio, R. J. Schoelkopf, M. Mirrahimi, and M. H. Devoret, *Confining the state of light to a quantum manifold by engineered two-photon loss*, *Science* **347**, 853 (2015).
- [62] P. Zapletal, A. Nunnenkamp, and M. Brunelli, *Stabilization of multimode schrödinger cat states via normal-mode dissipation engineering*, *PRX Quantum* **3**, 010301 (2022).
- [63] C. J. Myatt, B. E. King, Q. A. Turchette, C. A. Sackett, D. Kielpinski, W. M. Itano, C. Monroe, and D. J. Wineland, *Decoherence of quantum superpositions through coupling to engineered reservoirs*, *Nature* **403**, 269 (2000).
- [64] Z.-y. Jin and J. Jing, *Universal perspective on nonadiabatic quantum control*, *Phys. Rev. A* **111**, 012406 (2025).
- [65] Z.-y. Jin and J. Jing, *Universal quantum control by non-hermitian hamiltonian*, *Phys. Rev. A* **112**, 032605 (2025).
- [66] Z.-y. Jin and J. Jing, *Universal quantum control over bosonic networks*, *Phys. Rev. A* **113**, 012426 (2026).
- [67] Z.-y. Jin and J. Jing, *Universal quantum control over non-hermitian continuous-variable systems*, *Phys. Rev. A* **113**, 042452 (2026).
- [68] Z.-y. Jin, J. Q. You, and J. Jing, *From liouville equation to universal quantum control: A study of generating ultra highly squeezed states*, [arXiv:2604.02635](https://arxiv.org/abs/2604.02635) (2026).
- [69] J. Zhang, T. H. Kyaw, S. Filipp, L.-C. Kwek, E. Sjöqvist, and D. Tong, *Geometric and holonomic quantum computation*, *Phys. Rep.* **1027**, 1 (2023).
- [70] P.-R. Han, W. Ning, X.-J. Huang, R.-H. Zheng, S.-B. Yang, F. Wu, Z.-B. Yang, Q.-P. Su, C.-P. Yang, and S.-B. Zheng, *Measuring topological invariants for higher-order exceptional points in quantum three-mode systems*, *Nat. Commun.* **15**, 10293 (2024).
- [71] A. Metelmann and A. A. Clerk, *Nonreciprocal photon transmission and amplification via reservoir engineering*, *Phys. Rev. X* **5**, 021025 (2015).
- [72] Y.-P. Wang, J. W. Rao, Y. Yang, P.-C. Xu, Y. S. Gui, B. M. Yao, J. Q. You, and C.-M. Hu, *Nonreciprocity and unidirectional invisibility in cavity magnonics*, *Phys. Rev. Lett.* **123**, 127202 (2019).
- [73] D. C. Brody, *Biorthogonal quantum mechanics*, *J. Phys. A: Math. Theor.* **47**, 035305 (2013).
- [74] P.-M. Billangeon, J. S. Tsai, and Y. Nakamura, *Circuit-qed-based scalable architectures for quantum information processing with superconducting qubits*, *Phys. Rev. B* **91**, 094517 (2015).
- [75] N. Didier, J. Bourassa, and A. Blais, *Fast quantum nondemolition readout by parametric modulation of longitudinal qubit-oscillator interaction*, *Phys. Rev. Lett.* **115**, 203601 (2015).
- [76] S. Richer and D. DiVincenzo, *Circuit design implementing longitudinal coupling: A scalable scheme for superconducting qubits*, *Phys. Rev. B* **93**, 134501 (2016).
- [77] B. Royer, A. L. Grimsmo, N. Didier, and A. Blais, *Fast and high-fidelity entangling gate through parametrically modulated longitudinal coupling*, *Quantum* **1**, 11 (2017).
- [78] S. P. Harvey, C. G. L. Böttcher, L. A. Orona, S. D. Bartlett, A. C. Doherty, and A. Yacoby, *Coupling two spin qubits with a high-impedance resonator*, *Phys. Rev. B* **97**, 235409 (2018).
- [79] C. G. L. Böttcher, S. P. Harvey, S. Fallahi, G. C. Gardner, M. J. Manfra, U. Vool, S. D. Bartlett, and A. Yacoby, *Parametric longitudinal coupling between a high-impedance superconducting resonator and a semiconductor quantum dot singlet-triplet spin qubit*, *Nat. Commun.* **13**, 4773 (2022).
- [80] S. Bosco, P. Scarlino, J. Klinovaja, and D. Loss, *Fully tunable longitudinal spin-photon interactions in si and ge quantum dots*, *Phys. Rev. Lett.* **129**, 066801 (2022).
- [81] A. Blais, R.-S. Huang, A. Wallraff, S. M. Girvin, and R. J. Schoelkopf, *Cavity quantum electrodynamics for superconducting electrical circuits: An architecture for quantum computation*, *Phys. Rev. A* **69**, 062320 (2004).
- [82] D. I. Schuster, A. Wallraff, A. Blais, L. Frunzio, R.-S. Huang, J. Majer, S. M. Girvin, and R. J. Schoelkopf, *ac stark shift and dephasing of a superconducting qubit strongly coupled to a cavity field*, *Phys. Rev. Lett.* **94**, 123602 (2005).
- [83] A. Wallraff, D. I. Schuster, A. Blais, L. Frunzio, J. Majer, M. H. Devoret, S. M. Girvin, and R. J. Schoelkopf, *Approaching unit visibility for control of a superconducting qubit with dispersive readout*, *Phys. Rev. Lett.* **95**, 060501 (2005).
- [84] M. Reagor, W. Pfaff, C. Axline, R. W. Heeres, N. Ofek, K. Sliwa, E. Holland, C. Wang, J. Blumoff, K. Chou, M. J. Hatridge, L. Frunzio, M. H. Devoret, L. Jiang, and R. J. Schoelkopf, *Quantum memory with millisecond coherence in circuit qed*, *Phys. Rev. B* **94**, 014506 (2016).
- [85] W. Wang, L. Hu, Y. Xu, K. Liu, Y. Ma, S.-B. Zheng, R. Vijay, Y. P. Song, L.-M. Duan, and L. Sun, *Converting quasiclassical states into arbitrary fock state superpositions in a superconducting circuit*, *Phys. Rev. Lett.* **118**, 223604 (2017).
- [86] I. Yang, T. Agrenius, V. Usova, O. Romero-Isart, and G. Kirchmair, *Hot schrödinger cat states*, *Sci. Adv.* **11**, eadr4492 (2025).
- [87] O. Katz and C. Monroe, *Programmable quantum simulations of bosonic systems with trapped ions*, *Phys. Rev. Lett.* **131**, 033604 (2023).
- [88] M. Lee, K. Friebe, D. A. Fioretto, K. Schüppert, F. R. Ong, D. Plankensteiner, V. Torggler, H. Ritsch, R. Blatt, and T. E. Northup, *Ion-based quantum sensor for optical cavity photon numbers*, *Phys. Rev. Lett.* **122**, 153603 (2019).